7.92 ± 0.12 m and 9.68 ± 0.19 m, respectively, for the modified blindfolded-walking tasks. The similarity between the results obtained from both types of walking task indicates that our modified walking task can also be used to accurately reflect the observer's distance judgement.

The perceptual matching task. The target viewing conditions were similar to those used for the walking task. To obtain the observer's perception of distance, the matching target was placed 90° from the observer. The observer's task was to view the test target, then turn toward the matching target and instruct the experimenter to adjust the location of the matching target until it appeared to be at the same distance from him as the test target.

Each observer underwent a practice session before commencing the experiments. During the proper experiments, the observers were tested under the same condition two to three times, depending on the particular task. When more than one target distance was tested in an experiment, the order of testing was counterbalanced across observers.

Received 11 May; accepted 16 July 1998.

1. Shannon, C. E. & Weaver, W. *The Mathematical Theory of Communication* (Univ. Illinois Press, Urbana, 1949).
2. Gibson, J. J. *The Perception of the Visual World* (Houghton Mifflin, Boston, 1950).
3. Barlow, H. B. in *Sensory Communication* (ed. Rosenblith, W.) 217–235 (MIT Press, Cambridge, Massachusetts, 1961).
4. Attneave, F. Informational aspects of visual perception. *Psychol. Rev.* **61,** 183–193 (1954).
5. Sedgwick, H. A. in *Human and Machine Vision* (eds Rosenthal, A. & Beck, J.) 425–458 (Academic, New York, 1983).
6. Thomson, J. A. Is continuous visual monitoring necessary in visually guided locomotion? *J. Exp. Psychol. Hum. Percept. Perform.* **9,** 427–443 (1983).
7. Elliot, D. Continuous visual information may be important after all: a failure to replicate Thomson (1983). *J. Exp. Psychol. Hum. Percept. Perform.* **12,** 388–391 (1987).
8. Steenuis, R. E. & Goodale, M. A. The effects of time and distance on accuracy of target-directed locomotion: does an accurate short-term memory for spatial location exist? *J. Motor Behav.* **20,** 399–415 (1988).
9. Rieser, J. J., Ashmead, D. H., Talor, C. R. & Youngquist, G. A. Visual perception and the guidance of locomotion without vision to previously seen targets. *Perception* **19,** 675–689 (1990).
10. Loomis, J., DaSilva, J., Fujita, N. & Fukusima, S. Visual space perception and visually directed action. *J. Exp. Psychol.* **18,** 906–921 (1992).
11. Loomis, J., DaSilva, J., Philbeck, J. W. & Fukusima, S. Visual perception of location and distance. *Curr. Dir. Psychol. Sci.* **5,** 72–77 (1996).
12. Jiang, Y. & Mark, L. S. The effect of gap depth on the perception of whether a gap is crossable. *Percept. Psychophys.* **56,** 691–700 (1994).
13. Philbeck, J. W. & Loomis, J. M. Comparison of two indicators of perceived egocentric distance under full-cue and reduced-cue conditions. *J. Exp. Psychol. Hum. Percept. Perform.* **23,** 72–85 (1997).
14. Cutting, J. E. & Vishton, P. M. in *Handbook of Perception and Cognition: Perception of Space and Motion* Vol. 6 (eds Epstein, W. & Rogers, S.) 69–117 (Academic, San Diego, 1995).
15. Mark, L. S. Eye-height scaled information about affordances: a study of sitting and stair climbing. *J. Exp. Psychol. Hum. Percept. Perform.* **13,** 360–370 (1987).
16. Warren, W. H. & Whang, S. Visual guidance of walking through apertures: body-scaled information for affordances. *J. Exp. Psychol. Hum. Percept. Perform.* **13,** 371–383 (1987).
17. Sedgwick, H. A. Combining multiple forms of visual information to specify contact relations in spatial layout. *SPIE* **1198,** 447–458 (1989).
18. He, J. Z. & Nakayama, K. Apparent motion determined by surface layout not by disparity or by 3-dimensional distance. *Nature* **367,** 173–175 (1994).

Acknowledgements. This research was supported in part by a Sloan Research Fellowship from the Alfred P. Sloan Foundation (to Z.J.H.) and by a Faculty Research Grant from SCO (to T.L.O.).

Correspondence and requests for materials should be addressed to Z.J.H. (e-mail: z0he0002@ulkyvm.louisville.edu).

Shape selectivity in primate lateral intraparietal cortex

A. B. Sereno*† & J. H. R. Maunsell*‡

* *Division of Neuroscience S-603 and ‡ Howard Hughes Medical Institute, Baylor College of Medicine, Houston, Texas 77030, USA*

† *Center for Molecular and Behavioral Neuroscience, Rutgers University, Newark, New Jersey 07102, USA*

The extrastriate visual cortex can be divided into functionally distinct temporal and parietal regions, which have been implicated in feature-related ('what') and spatial ('where') vision, respectively[1]. Neuropsychological studies of patients with damage to either the temporal or the parietal regions provide support for this functional distinction[2–4]. Given the prevailing modular theoretical framework and the fact that prefrontal cortex receives inputs from both temporal and parietal streams[5,6], recent studies have focused on the role of prefrontal cortex in understanding where and how information about object identity is integrated with (or remains segregated from) information about object location[7–10]. Here we show that many neurons in primate posterior parietal cortex (the 'where' pathway) show sensory shape selectivities to simple, two-dimensional geometric shapes while the animal performs a simple fixation task. In a delayed match-to-sample paradigm, many neuronal units also show significant differences in delay-period activity, and these differences depend on the shape of the sample. These results indicate that units in posterior parietal cortex contribute to attending to and remembering shape features in a way that is independent of eye movements, reaching, or object manipulation. These units show shape selectivity equivalent to any shown in the ventral pathway.

Previous studies of the parietal cortex that demonstrated its sensitivity to object shape have tended to focus on tasks involving hand manipulation of three-dimensional solid objects[11–14]. Little attention, however, has been paid to the basic question of simple, two-dimensional shape selectivity in the parietal cortex. Here we test directly the extent to which units in the lateral intraparietal area (LIP) in posterior parietal cortex respond to differently shaped, two-dimensional visual stimuli that the animal did not and could not manipulate.

We recorded from 124 isolated neurons in area LIP of two macaque monkeys. The monkeys were trained to perform a simple fixation task. After the animal fixated a central spot, a shape was briefly presented within the receptive field of the unit being recorded. We recorded the activity of 74 of the 124 neurons while the animal performed this fixation task. Surprisingly, many units (42 of 74, 57%) showed a significant difference in activity during the stimulus presentation, which was dependent on which of eight shapes was presented (Fig. 1).

We calculated a shape-selectivity index (SI) for each unit using the average rate of firing for the stimuli that produced the strongest and weakest responses ($SI = (max - min)/(max + min)$). The histogram in Fig. 2 shows the distribution of indices, with units that show significant differences in responses to different shapes being indicated in black. The median of the indices for these significant units corresponded to a response that was 2.5 times stronger for the most-preferred (best) relative to the least-preferred (worst) shape (median $SI = 0.43$).

This shape selectivity is unlikely to arise from accidental interactions between shape features and receptive-field profiles, because LIP receptive fields are typically large and homogeneous[15]. Nevertheless, to discount such accidental interactions, we tested some units using stimuli in different positions or of different sizes. For 6 of the 42 units with significant differences in response that were dependent on the shape of the stimulus, the same stimuli were presented at the same eccentricity in a second location. The polar angular difference between the first and second location ranged from 25 to 130 degrees depending on the size of the receptive field of the particular unit. There was good agreement between the shape selectivities in the two locations. For three of the units, the preferred shape or preferred two shapes in one location were the same in the second location. For the remaining three units, which were more broadly tuned, at least one or two of the three shapes with the strongest response agreed. In addition, the least-preferred one or two shapes in one location remained the same in the second location. For two units with significant sensitivity to shape, we recorded the activity of each unit when the size of the stimuli was increased by 50%. Each unit maintained its shape preference. These results indicate that shape selectivities in LIP units are not an accidental result of receptive-field profiles.

To test for shape-selective behavioural effects in area LIP, we trained the animals on a delayed match-to-sample task. After the monkey fixated a central spot, a sample shape was briefly presented in one of three eccentric locations. After a short delay (0.5–2.1 s),

three test shapes appeared simultaneously. The animal had to make a saccade to the test shape that matched the sample shape, regardless of sample and test-stimulus locations. Many units (41 of 124 units, 33%) showed a significant difference in activity during the delay period depending on the shape of the sample (Fig. 3). Such selective activation probably contributes to the animal's ability to attend to and remember the sample shape during the period in which no stimulus is on the screen.

For the most responsive location of each unit during the delay period, we calculated a shape-selectivity index by dividing the average spike-rate difference of the shape with the greatest delay activity (max) and the shape with the weakest delay activity (min) by the sum of their average spike rates. The histogram in Fig. 4 represents the population of units. Units with significant shape-dependent differences in delay activity are indicated in black. These units showed a 73% increase in firing rate for the most-preferred (best) shape compared with the least-preferred (worst) shape (median SI = 0.27).

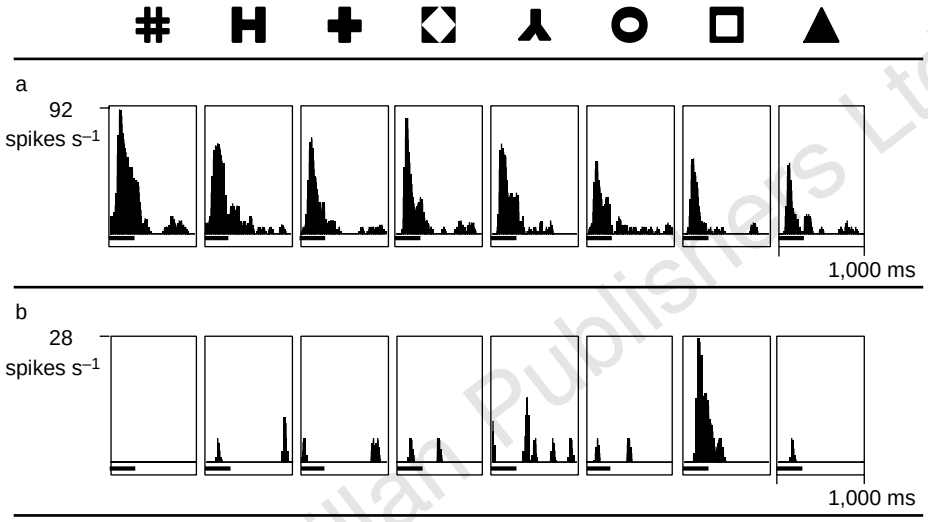

Figure 1 Responses of two neurons during the passive fixation task. **a**, Broadly tuned, shape-selective sensory response (SI = 0.40). **b**, Narrowly tuned, shape-selective sensory response (SI = 0.83). Peristimulus-time histograms from each of two neurons for all eight stimulus conditions are presented with the corresponding shape indicated above its respective histograms. Each histogram shows the activity of the neuron during the stimulus period (horizontal bar) and the fixation period that followed for each of six trials (**a**) or five trials (**b**). For the unit in **a**, the histograms corresponding to the different shape conditions are ordered by decreasing magnitude of activity during the sample stimulus period.

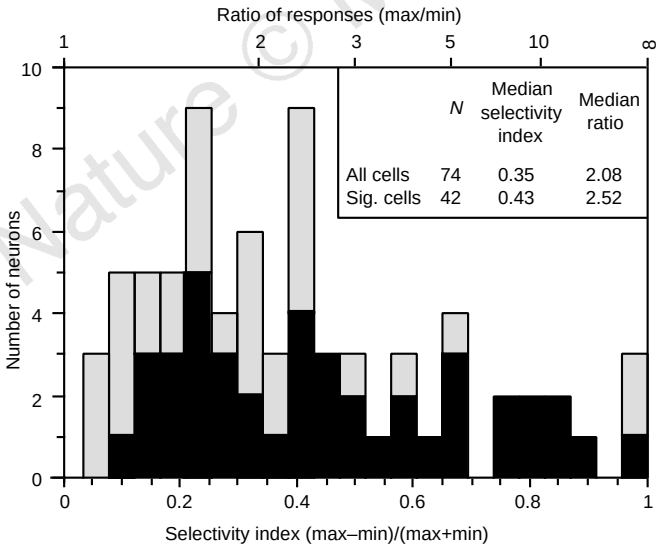

Figure 2 Histogram showing the magnitude of the sensory shape selectivity during the passive fixation task the population of units recorded. Units with significant shape-dependent differences in sample activity are indicated in black. The median selectivity index for the significant units was 0.43.

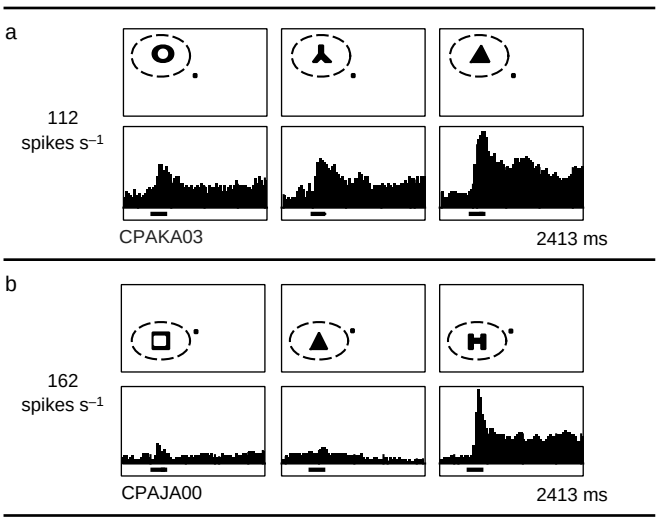

Figure 3 Responses of two neurons during the delayed match-to-sample task. **a**, Broadly tuned, shape-selective delay-period activity. **b**, Narrowly tuned, shape-selective, delay-period activity. Peristimulus-time histograms from a neuron for three particular sample stimulus conditions are presented. The dashed oval represents the neuron's receptive field. Each histogram was compiled from 12 trials and shows the activity of the neuron during the presample fixation period, the sample period (horizontal bar), and the delay period. These neurons show shape selectivity during both the sample and the delay periods. Although only the fixation spot (small black square) was present during the delay period for all three conditions, the neuron in (**b**) was much more active when the sample H-shape had been presented inside its receptive field.

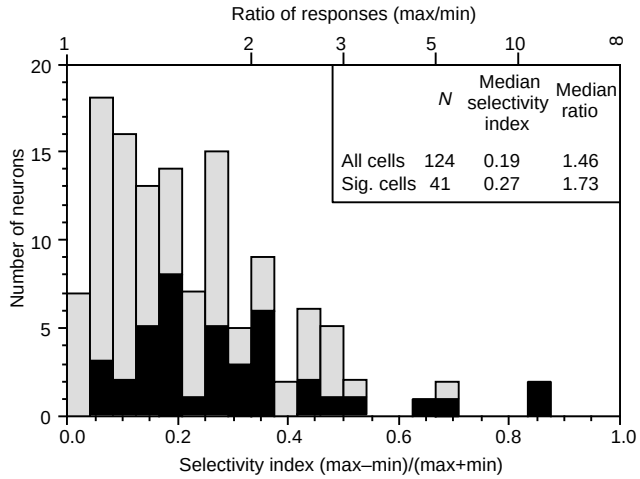

Figure 4 Histogram showing the magnitude of the delay-period shape selectivity during the match-to-sample task for the population of units recorded. Units with significant shape-dependent differences in delay-period activity are indicated in black. The median selectivity index for the significant units was 0.27. Although, for many units, we attempted to include the shapes that seemed to produce the best and worst response among the three shapes used in the task, it is possible that, compared with the sensory shape effects reported above using all eight shapes, we may have underestimated the delay-period shape effects.

Although LIP is important for spatial perception, it represents a late stage in visual processing and has strong associations with structures involved in the planning and execution of eye movements[16]. Thus there is much debate over whether units in LIP, and in posterior parietal cortex more generally, represent the spatial whereabouts of objects, or whether they guide parts of the body to the location that these objects occupy[17–19]. The latter view, which takes into account the output requirements of the 'where' pathway, has been put forward to explain shape selectivity in the 'where' pathway. For example, neurons in the anterior intraparietal area can be sensitive to those visual qualities of an object that determine the posture of the hand and fingers during a grasping movement[20–22].

However, our results present problems for a strictly intentional view of the function of posterior parietal cortex[23]. Many LIP units showed changes in response to different shapes presented in their receptive field that could not be accounted for by different eye movements. Most units also showed shape selectivities even in a passive fixation task. The shape selectivity we report in LIP presents an enigma. Because different shapes are presented in the same location, it is difficult to see how they entail different eye-movement programming, whether or not the animal makes an eye movement. Moreover, shape selectivity in LIP is consistent with anatomical studies showing that LIP receives projections from areas in the 'what' pathway, including areas V4, TEO and TE (ref. 6). Neurophysiological studies also indicate that the temporal waveforms of neuronal discharge in LIP may contain information that can be used to discriminate stimulus patterns[24,25]. Shape selectivity in the 'where' pathway is a relatively unexplored frontier that promises to change our understanding of cortical visual processing. □

Methods

Tasks and procedures. During the passive fixation task, the stimulus shape was positioned so that it fell within the receptive field. The stimulus for each trial was selected from a set of eight different shapes. Each was a simple two-dimensional black-and-white geometric form (Fig. 1). Each shape fit within the same-sized square region and had an equal number of bright pixels. All eight shapes were centred on the same position within the unit's receptive field. In each trial, the randomly selected shape was presented four times before a central fixation spot was extinguished. Each repetition of the shape was presented for a constant duration, ranging from 250 to 300 ms among the units recorded. Likewise, each interstimulus interval was of constant duration, ranging from 500 to 750 ms. The animals were required to maintain fixation within 0.5° of the central 0.1° spot in the centre of the video display throughout the trial. Eye position was monitored using the scleral search-coil method. The animals were rewarded for maintaining fixation on the central spot until it disappeared. For most of the units recorded, stimulus eccentricity ranged between 3.5° and 6.0° and stimulus size ranged between 0.4° and 0.8°.

During the delayed match-to-sample task, after the animal fixated a 0.1° spot in the centre of the video display, a sample shape was presented (ranging from 200 to 400 ms among the units recorded) in one of three locations. The sample was immediately followed by a full-screen pattern mask (duration 15 ms), followed by a variable delay period, ranging from 500 to 2,100 ms among the units recorded. Finally, a test array of three shapes appeared, equidistant from the fixation spot. The animal was required to make an eye movement to the test shape that matched the sample shape for a juice reward. For each unit, samples and test stimuli were a subset of three of eight different shapes (Fig. 1). For most units, the two shapes that elicited the strongest response and the one shape that elicited the weakest response were selected. In catch trials (up to 20% of trials), the test array did not include the sample shape, which was replaced instead by one of the five other shapes. In these trials, the animal was rewarded for maintaining fixation on the central spot until it disappeared (an additional 1,300–1,900 ms). The stimulus arrays were configured so that at least one stimulus position fell within the receptive field. For most of the units recorded, stimulus eccentricity ranged between 3.5° and 6.0° and stimulus size ranged between 0.4° and 0.8°.

Histology. In one animal, histological reconstruction showed, on the basis of myeloarchitectonic criteria[16,26], that the 85 units recorded in the lateral bank of the intraparietal sulcus lay within area LIP.

Data analysis. For statistical analysis in the passive fixation task, an *F*-test for shape selectivity was performed on the average rate of firing for the eight different shapes during the sample period, starting 50 ms poststimulus (collapsed across repetitions within as well as across trials). For statistical analysis in the delayed match-to-sample task, an *F*-test was performed on the average rate of firing during the last 300 ms of the delay period. For all statistical tests, a significant criterion level of $P < 0.05$ was used.

Received 1 June; accepted 23 July 1998.

1. Ungerleider, L. G. & Mishkin, M. in *The Analysis of Visual Behavior* (eds Ingle, D. J., Goodale, M. A. & Mansfield, R. J. W.) 549–586 (MIT Press, Cambridge, MA, 1982).
2. Goodale, M. A. & Milner, A. D. Separate visual pathways for perception and action. *Trends Neurosci.* **15,** 20–25 (1992).
3. Farah, M. J. *Visual Agnosia* (MIT Press, Cambridge, MA, 1990).
4. Perenin, M. & Vighetto, A. Optic ataxia: a specific disruption in visuomotor mechanisms. I. Different aspects of the deficit in reaching for objects. *Brain* **111,** 643–674 (1988).
5. Cavada, C. & Goldman-Rakic, P. S. Posterior parietal cortex in rhesus monkey: II. Evidence for segregated corticocortical networks linking sensory and limbic areas with the frontal lobe. *J. Comp. Neurol.* **287,** 422–445 (1989).
6. Webster, M. J., Bachevalier, J. & Ungerleider, L. G. Connections of inferior temporal areas TEO and TE with parietal and frontal cortex in macaque. *Cerebral Cortex* **5,** 470–483 (1994).
7. Wilson, F. A. W., O Scalaidhe, S. P. & Goldman-Rakic, P. S. Dissociation of object and spatial processing domains in primate prefrontal cortex. *Science* **260,** 1955–1958 (1993).
8. Rao, C. S., Rainer, G. & Miller, E. K. Integration of what and where in the primate prefrontal cortex. *Science* **276,** 821–824 (1997).
9. O Scalaidhe, S. P., Wilson, F. A. W. & Goldman-Rakic, P. S. Areal segregation of face-processing neurons in prefrontal cortex. *Science* **278,** 1135–1138 (1997).
10. Courtney, S. M., Petit, L., Maisog, J. M., Ungerleider, L. G. & Haxby, J. V. An area specialized for spatial working memory in human frontal cortex. *Science* **279,** 1347–1351 (1998).
11. Taira, M., Mine, S., Georgopoulos, A. P., Murata, A. & Sakata, H. Parietal cortex neurons of the monkey related to the visual guidance of hand movement. *Exp. Brain Res.* **83,** 29–36 (1990).
12. Murata, A., Gallese, V., Kaseda, M. & Sakata, H. Parietal neurons related to memory-guided hand manipulation. *J. Neurophysiol.* **75,** 2180–2186 (1996).
13. Jeannerod, M. The formation of finger grip during prehension. A cortically mediated visuomotor pattern. *Behav. Brain Res.* **19,** 99–116 (1986).
14. Gallese, V., Murata, A., Kaseda, M., Niki, N. & Sakata, H. Deficit of hand preshaping after muscimol injection in monkey parietal cortex. *Neuroreport* **5,** 1525–1529 (1994).
15. Barash, S., Bracewell, R. M., Fogassi, L., Gnadt, J. W. & Andersen, R. A. Saccade-related activity in the lateral intraparietal area II. Spatial properties. *J. Neurophysiol.* **66,** 1109–1124 (1991).
16. Andersen, R. A., Asanuma, C., Essick, G. & Seigel, R. M. Corticocortical connections of anatomically and physiologically defined subdivisions within the inferior parietal lobule. *J. Comp. Neurol.* **296,** 65–113 (1990).
17. Shadlen, M. Look but don't touch, or vice versa. *Nature* **386,** 122–123 (1997).
18. Rizzolatti, G., Riggio, L. & Sheliga, B. M. in *Attention and Performance XV* (eds Umiltà, C. & Moscovitch, M.) 231–265 (MIT Press, Cambridge, MA, 1994).
19. Colby, C. L. Action-oriented spatial reference frames in cortex. *Neuron* **20,** 15–24 (1998).
20. Goodale, M. A. *et al.* Separate neural pathways for the visual analysis of object shape in perception and prehension. *Curr. Biol.* **4,** 604–610 (1994).
21. Jeannerod, M., Arbib, M. A., Rizzolatti, G. & Sakata, H. Grasping objects: the cortical mechanisms of visuomotor transformation. *Trends Neurosci.* **18,** 314–320 (1995).

22. Sakata, H., Taira, M., Murata, A. & Mine, S. Neural mechanisms of visual guidance of hand action in the parietal cortex of the monkey. *Cerebr. Cortex* **5,** 429–438 (1995).
23. Snyder, L. H., Batista, A. P. & Andersen, R. A. Coding of intention in the posterior parietal cortex. *Nature* **386,** 167–170 (1997).
24. Goldberg, M. E. & Gottlieb, J. Neurons in monkey LIP transmit information about stimulus pattern in the temporal waveform of their discharge. *Soc. Neurosci. Abstr.* **23,** 17 (1997).
25. Troscianko, T. *et al*. Human colour discrimination based on a non-parvocellular pathway. *Curr. Biol.* **6,** 200–210 (1996).
26. Blatt, G. J., Andersen, R. A. & Stoner, G. R. Visual receptive field organization and cortico-cortical connections of the lateral intraparietal area (area LIP) in the macaque. *J. Comp. Neurol.* **299,** 421–445 (1990).

Acknowledgements. We thank K. Briand, R. Klein, S. Lehky and S. O Scalaidhe for comments on the manuscript. This work was supported by awards from the McDonnell–Pew Foundation, NARSAD, NIMH, and NEI. J.H.R.M. is an Investigator with the Howard Hughes Medical Institute. Animal experiments were conducted in accordance with the Baylor College of Medicine and Rutgers University Animal Care Committees.

Correspondence and requests for materials should be addressed to A.B.S. (e-mail: sereno@cmbn.rutgers.edu).

Mechanism of calcium gating in small-conductance calcium-activated potassium channels

X.-M. Xia*, B. Fakler†, A. Rivard*, G. Wayman*, T. Johnson-Pais*, J. E. Keen*, T. Ishii*, B. Hirschberg*, C. T. Bond*, S. Lutsenko‡, J. Maylie§ & J. P. Adelman*

** Vollum Institute, Departments of ‡ Biochemsitry and Molecular Biology, and § Obstetrics and Gynecology, Oregon Health Sciences University, Portland, Oregon 97201, USA*
† Department of Physiology, University of Tuebingen, Tuebingen, Germany

The slow afterhyperpolarization that follows an action potential is generated by the activation of small-conductance calcium-activated potassium channels (SK channels). The slow afterhyperpolarization limits the firing frequency of repetitive action potentials (spike-frequency adaption) and is essential for normal neurotransmission[1–3]. SK channels are voltage-independent and activated by submicromolar concentrations of intracellular calcium[1]. They are high-affinity calcium sensors that transduce fluctuations in intracellular calcium concentrations into changes in membrane potential. Here we study the mechanism of calcium gating and find that SK channels are not gated by calcium binding directly to the channel α-subunits. Instead, the functional SK channels are heteromeric complexes with calmodulin, which is constitutively associated with the α-subunits in a calcium-independent manner. Our data support a model in which calcium gating of SK channels is mediated by binding of calcium to calmodulin and subsequent conformational alterations in the channel protein.

Calcium ions are ubiquitous regulators of many cellular processes, and eukaryotic cells have evolved a complex system of transmembrane molecules, channels, pumps and exchangers, which maintain intracellular Ca^{2+} concentrations at very low levels, 10–100 nM. This allows rapid metabolic responses to Ca^{2+} fluxes[4,5]. Several classes of ion channels, such as Ca^{2+}-activated potassium channels, are gated by intracellular Ca^{2+} ions, thereby coupling intracellular Ca^{2+} levels and membrane potential.

The genes encoding a family of SK channels have been cloned. The amino-acid sequences of the three known members of the SK-channel family, SK1, SK2 and SK3, show that the channels share high overall structural homology, with little similarity to members of other potassium-channel subfamilies[6]. Because of the fundamental role played by SK channels in regulating neuronal excitability, we studied the mechanism underlying Ca^{2+} gating of SK channels.

Current recordings from giant inside-out patches of *Xenopus* oocytes showed that all SK-channel subtypes exhibit similar Ca^{2+} dose–response relationships, with Ca^{2+} concentrations required for half-maximal activation ($K_{0.5}$) of ~0.3 μM and a Hill coefficient of ~4 (Fig. 1a). Fast piezo-driven application of Ca^{2+} (10 μM) showed that onset of current commences within 1 ms, with time constants of activation of 5–15 ms (Fig. 1b–d). This rate is similar to that for the rapid activation of ligand-gated ion channels[7,8]. SK currents could be repeatedly activated in continuously perfused patches for as long as the patches remained intact without changes in the activation kinetics, and application of protein kinase inhibitors (W7 or H89) or phosphatase inhibitors (okadaic acid) did not affect Ca^{2+} gating (results not shown). ATP and other nucleotides were not present in the intracellular solution. These results indicate that no diffusable second messengers or protein kinases are necessary for SK-channel gating, and that gating reflects interactions between the channel and Ca^{2+} only.

The similarity in the nature of Ca^{2+} gating of the three SK channels indicates that the structural elements underlying Ca^{2+} gating are conserved. The submicromolar affinity for Ca^{2+} is reminiscent of the affinity for Ca^{2+} of an EF-hand Ca^{2+}-binding protein[9], yet no such motif is present in the SK channels, nor are C2 domains[10] or motifs similar to the 'calcium bowl' present in BK channels[11]. However, if Ca^{2+} ions are directly chelated by the channel protein then, as for other known Ca^{2+}-binding motifs, negatively charged residues, glutamate and aspartate, are likely to mediate Ca^{2+} binding. Therefore, each of the 21 conserved negatively charged residues within the predicted intracellular domains of the SK-channel α-subunits (Fig. 2a) was mutated individually into a neutral amino acid (E → Q, D → N) in the SK2 channel. Dose–response experiments showed that in no case was Ca^{2+} gating markedly altered (Fig. 2b). In addition, we made two mutant subunits, one containing neturalizations of the four conserved negatively charged residues in the loop connecting transmembrane domains 2 and 3 (2–3 loop), and the other containing neutralizations of the first nine conserved negatively charged residues in the carboxy terminus. Expression of the 2–3-loop mutant resulted in normal, Ca^{2+}-dependent gating, whereas expression of the C-terminal mutant did not give rise to functional channels (Fig. 2c,d), indicating that the proximal part of the C terminus is

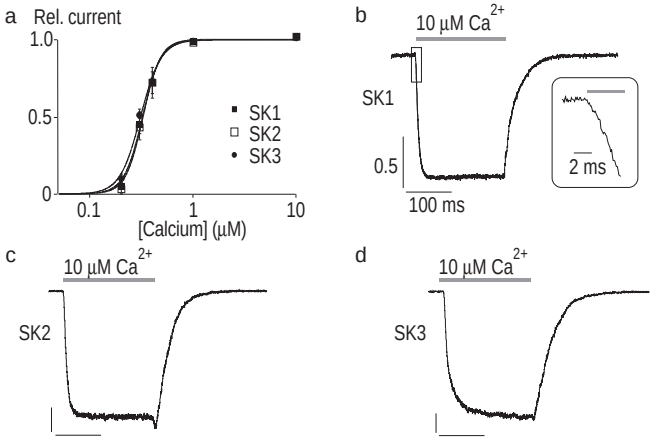

Figure 1 Ca^{2+} gating in SK channels. **a**, Ca^{2+} dose–response relationship for SK1, SK2 and SK3 channels. Relative current amplitude measured at –100 mV is plotted as a function of Ca^{2+} concentration. The data were fitted with the Hill equation, yielding $K_{0.5}$ and Hill coefficient of 0.31 ± 0.01 μM and 4.4 ± 0.2, 0.33 μM ± 0.01 and 5.3 ± 0.9, and 0.32 ± 0.03 μM and 5.0 ± 0.6 for SK1, 2 and 3, respectively. **b**–**d**, Fast piezo-driven application of Ca^{2+} (10 μM) to inside-out patches expressing SK1 (**b**), SK2 (**c**), or SK3 (**d**) channels. The holding potential was –80 mV; current and time calibrations are 0.5 nA and 100 ms. Inset for SK1 shows a current increase within 1 ms after Ca^{2+} application. Time constants for activation and deactivation, determined from mono-exponential fits, were 5.8, 6.3 and 12.9 ms for activation and 21.7, 29.6 and 38.1 ms for deactivation of SK1, SK2 and SK3, respectively.